Author/s:
Pal, B;Schwartz, AJ;Abdesselam, A;Adachi, I;Aihara, H;Al Said, S;Arinstein, K;Asner, DM;Aulchenko, V;Aushev, T;Ayad, R;Babu, V;Badhrees, I;Bakich, AM;Bobrov, A;Bonvicini, G;Bozek, A;Bračko, M;Browder, TE;Červenkov, D;Chang, MC;Chekelian, V;Chen, A;Cheon, BG;Cho, K;Chobanova, V;Choi, Y;Cinabro, D;Dalseno, J;Doležal, Z;Drásal, Z;Drutskoy, A;Dutta, D;Eidelman, S;Farhat, H;Fast, JE;Ferber, T;Frost, O;Fulsom, BG;Gaur, V;Gabyshev, N;Ganguly, S;Garmash, A;Getzkow, D;Gillard, R;Glattauer, R;Goh, YM;Golob, B;Grzymkowska, O;Hara, T;Hayasaka, K;Hayashii, H;He, XH;Hou, WS;Huschle, M;Hyun, HJ;Iijima, T;Ishikawa, A;Itoh, R;Iwasaki, Y;Jaegle, I;Julius, T;Kang, KH;Kato, E;Kiesling, C;Kim, DY;Kim, JB;Kim, JH;Kim, KT;Kim, MJ;Kim, SH;Kim, YJ;Kinoshita, K;Ko, BR;Kodyš, P;Korpar, S;Križan, P;Krokovny, P;Kuhr, T;Kumita, T;Kuzmin, A;Kwon, YJ;Lange, JS;Lee, DH;Lee, IS;Li, Y;Li Gioi, L;Libby, J;Liventsev, D;Lukin, P;Matvienko, D;Miyata, H;Mohanty, GB;Moll, A;Moon, HK;Nakamura, KR;Nakano, E;Nakao, M;Nanut, T;Natkaniec, Z

Title:
Evidence for the decay B0 →ηπ0

Date:
2015-07-09

Citation:
Pal, B., Schwartz, A. J., Abdesselam, A., Adachi, I., Aihara, H., Al Said, S., Arinstein, K., Asner, D. M., Aulchenko, V., Aushev, T., Ayad, R., Babu, V., Badhrees, I., Bakich, A. M., Bobrov, A., Bonvicini, G., Bozek, A., Bračko, M., Browder, T. E. ,... Natkaniec, Z. (2015). Evidence for the decay B0 →ηπ0. Physical Review D Particles Fields Gravitation and Cosmology, 92 (1), https://doi.org/10.1103/PhysRevD.92.011101.

Persistent Link:
https://hdl.handle.net/11343/194088

Belle Preprint 2015-2
KEK Preprint 2014-45
UCHEP Preprint 2015-2

Evidence for the decay $B^0 \to \eta\pi^0$

B. Pal,[6] A. J. Schwartz,[6] A. Abdesselam,[56] I. Adachi,[13,10] H. Aihara,[61] S. Al Said,[56,27] K. Arinstein,[4] D. M. Asner,[49] V. Aulchenko,[4] T. Aushev,[38,22] R. Ayad,[56] V. Babu,[57] I. Badhrees,[56,26] A. M. Bakich,[55] A. Bobrov,[4] G. Bonvicini,[66] A. Bozek,[45] M. Bračko,[34,23] T. E. Browder,[12] D. Červenkov,[5] M.-C. Chang,[69] V. Chekelian,[35] A. Chen,[42] B. G. Cheon,[11] K. Cho,[28] V. Chobanova,[35] Y. Choi,[54] D. Cinabro,[66] J. Dalseno,[35,58] Z. Doležal,[5] Z. Drásal,[5] A. Drutskoy,[22,37] D. Dutta,[15] S. Eidelman,[4] H. Farhat,[66] J. E. Fast,[49] T. Ferber,[7] O. Frost,[7] B. G. Fulsom,[49] V. Gaur,[57] N. Gabyshev,[4] S. Ganguly,[66] A. Garmash,[4] D. Getzkow,[8] R. Gillard,[66] R. Glattauer,[19] Y. M. Goh,[11] B. Golob,[32,23] O. Grzymkowska,[45] T. Hara,[13,10] K. Hayasaka,[40] H. Hayashii,[41] X. H. He,[50] W.-S. Hou,[44] M. Huschle,[25] H. J. Hyun,[30] T. Iijima,[40,39] A. Ishikawa,[60] R. Itoh,[13,10] Y. Iwasaki,[13] I. Jaegle,[12] T. Julius,[36] K. H. Kang,[30] E. Kato,[60] C. Kiesling,[35] D. Y. Kim,[53] J. B. Kim,[29] J. H. Kim,[28] K. T. Kim,[29] M. J. Kim,[30] S. H. Kim,[11] Y. J. Kim,[28] K. Kinoshita,[6] B. R. Ko,[29] P. Kodyš,[5] S. Korpar,[34,23] P. Križan,[32,23] P. Krokovny,[4] T. Kuhr,[25] T. Kumita,[63] A. Kuzmin,[4] Y.-J. Kwon,[68] J. S. Lange,[8] D. H. Lee,[29] I. S. Lee,[11] Y. Li,[65] L. Li Gioi,[35] J. Libby,[16] D. Liventsev,[65] P. Lukin,[4] D. Matvienko,[4] H. Miyata,[46] G. B. Mohanty,[57] A. Moll,[35,58] H. K. Moon,[29] K. R. Nakamura,[13] E. Nakano,[48] M. Nakao,[13,10] T. Nanut,[23] Z. Natkaniec,[45] M. Nayak,[16] S. Nishida,[13,10] S. Ogawa,[59] S. Okuno,[24] P. Pakhlov,[22,37] G. Pakhlova,[38,22] C. W. Park,[54] H. Park,[30] T. K. Pedlar,[33] L. Pesántez,[3] M. Petrič,[23] L. E. Piilonen,[65] C. Pulvermacher,[25] E. Ribežl,[23] M. Ritter,[35] A. Rostomyan,[7] S. Ryu,[52] Y. Sakai,[13,10] S. Sandilya,[57] D. Santel,[6] L. Santelj,[13] T. Sanuki,[60] Y. Sato,[39] O. Schneider,[31] G. Schnell,[1,14] C. Schwanda,[19] K. Senyo,[67] O. Seon,[39] M. E. Sevior,[36] M. Shapkin,[20] V. Shebalin,[4] C. P. Shen,[2] T.-A. Shibata,[62] J.-G. Shiu,[44] A. Sibidanov,[55] F. Simon,[35,58] Y.-S. Sohn,[68] E. Solovieva,[22] S. Stanič,[47] M. Starič,[23] M. Sumihama,[9] K. Sumisawa,[13,10] T. Sumiyoshi,[63] U. Tamponi,[21,64] Y. Teramoto,[48] F. Thorne,[19] M. Uchida,[62] S. Uehara,[13,10] Y. Unno,[11] S. Uno,[13,10] Y. Usov,[4] C. Van Hulse,[1] P. Vanhoefer,[35] G. Varner,[12] A. Vinokurova,[4] V. Vorobyev,[4] A. Vossen,[17] M. N. Wagner,[8] C. H. Wang,[43] M.-Z. Wang,[44] P. Wang,[18] X. L. Wang,[65] Y. Watanabe,[24] E. Won,[29] H. Yamamoto,[60] J. Yamaoka,[49] S. Yashchenko,[7] Z. P. Zhang,[51] V. Zhilich,[4] V. Zhulanov,[4] and A. Zupanc[23]

(The Belle Collaboration)

[1] *University of the Basque Country UPV/EHU, 48080 Bilbao*
[2] *Beihang University, Beijing 100191*
[3] *University of Bonn, 53115 Bonn*
[4] *Budker Institute of Nuclear Physics SB RAS and Novosibirsk State University, Novosibirsk 630090*
[5] *Faculty of Mathematics and Physics, Charles University, 121 16 Prague*
[6] *University of Cincinnati, Cincinnati, Ohio 45221*

[7]*Deutsches Elektronen–Synchrotron, 22607 Hamburg*
[8]*Justus-Liebig-Universität Gießen, 35392 Gießen*
[9]*Gifu University, Gifu 501-1193*
[10]*SOKENDAI (The Graduate University for Advanced Studies), Hayama 240-0193*
[11]*Hanyang University, Seoul 133-791*
[12]*University of Hawaii, Honolulu, Hawaii 96822*
[13]*High Energy Accelerator Research Organization (KEK), Tsukuba 305-0801*
[14]*IKERBASQUE, Basque Foundation for Science, 48013 Bilbao*
[15]*Indian Institute of Technology Guwahati, Assam 781039*
[16]*Indian Institute of Technology Madras, Chennai 600036*
[17]*Indiana University, Bloomington, Indiana 47408*
[18]*Institute of High Energy Physics,*
Chinese Academy of Sciences, Beijing 100049
[19]*Institute of High Energy Physics, Vienna 1050*
[20]*Institute for High Energy Physics, Protvino 142281*
[21]*INFN - Sezione di Torino, 10125 Torino*
[22]*Institute for Theoretical and Experimental Physics, Moscow 117218*
[23]*J. Stefan Institute, 1000 Ljubljana*
[24]*Kanagawa University, Yokohama 221-8686*
[25]*Institut für Experimentelle Kernphysik,*
Karlsruher Institut für Technologie, 76131 Karlsruhe
[26]*King Abdulaziz City for Science and Technology, Riyadh 11442*
[27]*Department of Physics, Faculty of Science,*
King Abdulaziz University, Jeddah 21589
[28]*Korea Institute of Science and Technology Information, Daejeon 305-806*
[29]*Korea University, Seoul 136-713*
[30]*Kyungpook National University, Daegu 702-701*
[31]*École Polytechnique Fédérale de Lausanne (EPFL), Lausanne 1015*
[32]*Faculty of Mathematics and Physics,*
University of Ljubljana, 1000 Ljubljana
[33]*Luther College, Decorah, Iowa 52101*
[34]*University of Maribor, 2000 Maribor*
[35]*Max-Planck-Institut für Physik, 80805 München*
[36]*School of Physics, University of Melbourne, Victoria 3010*
[37]*Moscow Physical Engineering Institute, Moscow 115409*
[38]*Moscow Institute of Physics and Technology, Moscow Region 141700*
[39]*Graduate School of Science, Nagoya University, Nagoya 464-8602*
[40]*Kobayashi-Maskawa Institute, Nagoya University, Nagoya 464-8602*
[41]*Nara Women's University, Nara 630-8506*
[42]*National Central University, Chung-li 32054*
[43]*National United University, Miao Li 36003*
[44]*Department of Physics, National Taiwan University, Taipei 10617*
[45]*H. Niewodniczanski Institute of Nuclear Physics, Krakow 31-342*
[46]*Niigata University, Niigata 950-2181*
[47]*University of Nova Gorica, 5000 Nova Gorica*
[48]*Osaka City University, Osaka 558-8585*
[49]*Pacific Northwest National Laboratory, Richland, Washington 99352*

[50] *Peking University, Beijing 100871*
[51] *University of Science and Technology of China, Hefei 230026*
[52] *Seoul National University, Seoul 151-742*
[53] *Soongsil University, Seoul 156-743*
[54] *Sungkyunkwan University, Suwon 440-746*
[55] *School of Physics, University of Sydney, NSW 2006*
[56] *Department of Physics, Faculty of Science, University of Tabuk, Tabuk 71451*
[57] *Tata Institute of Fundamental Research, Mumbai 400005*
[58] *Excellence Cluster Universe, Technische Universität München, 85748 Garching*
[59] *Toho University, Funabashi 274-8510*
[60] *Tohoku University, Sendai 980-8578*
[61] *Department of Physics, University of Tokyo, Tokyo 113-0033*
[62] *Tokyo Institute of Technology, Tokyo 152-8550*
[63] *Tokyo Metropolitan University, Tokyo 192-0397*
[64] *University of Torino, 10124 Torino*
[65] *CNP, Virginia Polytechnic Institute and State University, Blacksburg, Virginia 24061*
[66] *Wayne State University, Detroit, Michigan 48202*
[67] *Yamagata University, Yamagata 990-8560*
[68] *Yonsei University, Seoul 120-749*
[69] *Department of Physics, Fu Jen Catholic University, Taipei 24205*

Abstract

We report a search for the charmless hadronic decay $B^0 \to \eta\pi^0$ with a data sample corresponding to an integrated luminosity of 694 fb^{-1} containing 753×10^6 $B\overline{B}$ pairs. The data were collected by the Belle experiment running on the $\Upsilon(4S)$ resonance at the KEKB e^+e^- collider. We measure a branching fraction $\mathcal{B}(B^0 \to \eta\pi^0) = (4.1^{+1.7+0.5}_{-1.5-0.7}) \times 10^{-7}$, where the first uncertainty is statistical and the second is systematic. Our measurement gives an upper limit of $\mathcal{B}(B^0 \to \eta\pi^0) < 6.5 \times 10^{-7}$ at 90% confidence level. The signal has a significance of 3.0 standard deviations and constitutes the first evidence for this decay mode.

PACS numbers: 13.25.Hw, 12.15.Hh, 11.30.Er

Two-body charmless hadronic decays of B mesons are important for determining Standard Model parameters and for detecting the presence of new physics [1]. The decay $B^0 \to \eta\pi^0$ proceeds mainly via a $b \to u$ Cabibbo- and color-suppressed "tree" diagram, and via a $b \to d$ "penguin" diagram [2], as shown in Fig. 1. The branching fraction can be used to constrain isospin-breaking effects on the value of $\sin 2\phi_2$ ($\sin 2\alpha$) measured in $B \to \pi\pi$ decays [3, 4]. It can also be used to constrain CP-violating parameters ($C_{\eta' K}$ and $S_{\eta' K}$) governing the time dependence of $B^0 \to \eta' K^0$ decays [5]. The branching fraction is estimated using QCD factorization [6], soft collinear effective field theory [7], and flavor SU(3) symmetry [8] and is found to be in the range $(2 - 12) \times 10^{-7}$.

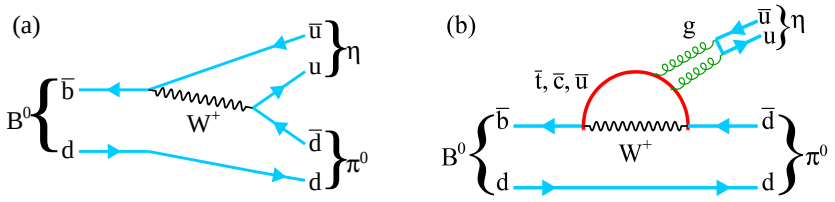

FIG. 1. (a) Tree and (b) penguin diagram contributions to $B^0 \to \eta\pi^0$.

Several experiments [9–13], including Belle, have searched for this decay mode. The current most stringent limit on the branching fraction is $\mathcal{B}(B^0 \to \eta\pi)^0 < 1.5 \times 10^{-6}$ at 90% confidence level (C.L.) [13]. Here we update our previous result [12] using the full data set of the Belle experiment running on the $\Upsilon(4S)$ resonance at the KEKB asymmetric-energy e^+e^- collider [14]. This data set corresponds to 753×10^6 $B\overline{B}$ pairs, which is a factor of 5 larger than that used previously. The analysis presented here also uses improved tracking, photon reconstruction, and continuum suppression algorithms.

The Belle detector is a large-solid-angle magnetic spectrometer consisting of a silicon vertex detector (SVD), a 50-layer central drift chamber (CDC), an array of aerogel threshold Cherenkov counters (ACC), a barrel-like arrangement of time-of-flight scintillation counters (TOF), and an electromagnetic calorimeter (ECL) comprising CsI(Tl) crystals. These detector components are located inside a superconducting solenoid coil that provides a 1.5 T magnetic field. An iron flux-return located outside the coil (KLM) is instrumented to detect K_L^0 mesons and to identify muons. Two inner detector configurations were used: a 2.0 cm beampipe and a three-layer SVD were used for the first 123 fb^{-1} of data, while a 1.5 cm beampipe, a four-layer SVD, and a small-cell inner drift chamber were used for the remaining 571 fb^{-1} of data. The detector is described in detail elsewhere [15, 16].

An ECL cluster not matched to any track is identified as a photon candidate. The timing of the energy deposited in the ECL must be consistent with the beam collision time identified at the trigger level. All photon candidates are required to have an energy greater than 50 MeV. We reconstruct $\pi^0 \to \gamma\gamma$ decays by pairing together photon candidates and requiring that the $\gamma\gamma$ invariant mass be in the range 0.115-0.155 GeV/c^2. This corresponds to $\pm 3.5\sigma$ around the nominal π^0 mass [17]. Photon candidates in the end cap regions are required to have an energy greater than 100 MeV for π^0 reconstruction. To improve the π^0 momentum resolution, we perform a mass-constrained fit and require that the resulting χ^2 be less than 50.

Candidate η mesons are reconstructed via $\eta \to \gamma\gamma$ ($\eta_{\gamma\gamma}$) and $\eta \to \pi^+\pi^-\pi^0$ ($\eta_{3\pi}$) decays. At least one of the photons in an $\eta_{\gamma\gamma}$ candidate must have an energy greater than 100 MeV.

To reduce combinatorial background from low-energy photons, $\eta_{\gamma\gamma}$ candidates are required to satisfy $|E_1-E_2|/(E_1+E_2) < 0.9$, where E_1 and E_2 are the two photon energies. Photons used for $\eta_{\gamma\gamma}$ reconstruction are not allowed to pair with any other photon to form a π^0 candidate. Candidate $\eta_{3\pi}$ mesons are reconstructed by combining a π^0 with a pair of oppositely charged tracks. These tracks are required to have a distance of closest approach with respect to the interaction point along the z axis (antiparallel to the e^+ beam) of $|dz| < 3.0$ cm, and in the transverse plane of $|dr| < 0.3$ cm. Pions are identified using information obtained from the CDC (dE/dx), the TOF, and the ACC. This information is combined to form a likelihood ($\mathcal{L}$) for hadron identification. We require that charged tracks satisfy $\mathcal{L}_K/(\mathcal{L}_\pi + \mathcal{L}_K) < 0.4$, where $\mathcal{L}_K\,(\mathcal{L}_\pi)$ is the likelihood of the track being a kaon (pion). We reject tracks whose response in the ECL and KLM are consistent with that of an electron or muon. The pion identification efficiency is 91.2% and the probability for a kaon to be misidentified as a pion is 5.4%. We require that the invariant mass of $\eta_{\gamma\gamma}$ and $\eta_{3\pi}$ candidates be in the ranges 0.500-0.575 GeV/c^2 and 0.538-0.557 GeV/c^2, respectively, corresponding to $\pm 2.5\sigma$ and $\pm 3.0\sigma$ in resolution around the nominal η mass [17]. For selected η candidates, a mass-constrained fit is performed to improve the momentum resolution.

Candidate B mesons are identified using the beam-energy-constrained mass, $M_{\rm bc} = \sqrt{E^2_{\rm beam} - |\vec{p}_B|^2c^2}/c^2$, and the energy difference, $\Delta E = E_B - E_{\rm beam}$, where $E_{\rm beam}$ is the beam energy, and E_B and $\vec{p}_B$ are the energy and momentum, respectively, of the B candidate. All quantities are evaluated in the $\Upsilon(4S)$ center-of-mass (CM) frame. We require that events satisfy $M_{\rm bc} > 5.24$ GeV/c^2 and -0.30 GeV $< \Delta E < 0.25$ GeV. We calculate signal yields in a smaller region $M_{\rm bc} > 5.27$ GeV/c^2 and -0.21 GeV $< \Delta E < 0.15$ GeV.

Charmless hadronic decays suffer from large backgrounds arising from continuum $e^+e^- \to q\bar{q}$ ($q = u, d, s, c$) production. To suppress this background, we use a multivariate analyzer based on a neural network (NN) [18]. The NN uses the event topology and B-flavor tagging information [19] to discriminate continuum events, which tend to be jetlike, from spherical $B\overline{B}$ events. The event shape variables include 16 modified Fox-Wolfram moments [20], the cosine of the angle between the z axis and the B flight direction, and the cosine of the angle between the thrust axis [21] of the B candidate and the thrust axis of the rest of the event. All quantities are evaluated in the $\Upsilon(4S)$ CM frame.

The NN technique requires a training procedure and, after training, achieves excellent separation between signal and background from the output variable C_{NB}. This variable ranges from -1 to $+1$: a value closer to -1 ($+1$) is more likely to identify a background (signal) event. The training samples used consist of Monte Carlo (MC) $B^0 \to \eta\pi^0$ events for signal and an $M_{\rm bc}$–ΔE sideband from data for background. The regions of 5.200 GeV/c^2 $< M_{\rm bc} <$ 5.265 GeV/c^2, $\Delta E < -0.23$ GeV and $\Delta E > 0.17$ GeV define the $M_{\rm bc}$–ΔE sideband. Independent samples are used to test the NN performance. The MC samples are obtained using EvtGen [22] for event generation and the Geant3 [23] package for modeling of the detector response. Final-state radiation is taken into account using the Photos [24] package.

We require $C_{NB} > -0.1$, which rejects approximately 85% of continuum background events while retaining 90% of signal events. We subsequently translate C_{NB} to C'_{NB}, defined as

$$C'_{NB} = \ln\left(\frac{C_{NB} - C^{\rm min}_{NB}}{C^{\rm max}_{NB} - C_{NB}}\right) \qquad (1)$$

where $C^{\rm min}_{NB} = -0.1$ and $C^{\rm max}_{NB}$ is the maximum value of C_{NB} obtained from a large sample of signal MC decays. This translation is advantageous as the C'_{NB} distribution for both signal

and background is well described by a sum of Gaussian functions.

After applying all selection criteria, 2% (7%) of events have more than one $B^0 \to \eta_{\gamma\gamma}\pi^0$ ($B^0 \to \eta_{3\pi}\pi^0$) candidate. For these events, we retain the $B^0 \to \eta\pi^0$ candidate with the smallest χ^2 value resulting from the η or, if necessary, π^0 mass-constrained fits. According to MC simulations, this criterion chooses the correct B candidate 63% (77%) of the time for $B^0 \to \eta_{\gamma\gamma}\pi^0$ ($B^0 \to \eta_{3\pi}\pi^0$).

We calculate signal yields using an unbinned extended maximum likelihood fit to the variables $M_{\rm bc}$, ΔE, and C'_{NB}. The likelihood function is defined as

$$\mathcal{L} = e^{-\sum_j Y_j} \cdot \prod_i^N \left(\sum_j Y_j \mathcal{P}_j(M_{\rm bc}^i, \Delta E^i, C_{NB}'^i) \right), \tag{2}$$

where N is the total number of events, $\mathcal{P}_j(M_{\rm bc}^i, \Delta E^i, C_{NB}'^i)$ is the probability density function (PDF) of signal or background component j for event i, and j runs over all signal and background components. Y_j is the yield of component j. The background components consist of $e^+e^- \to q\bar{q}$ continuum events, generic $b \to c$ processes, and charmless rare processes. The latter two backgrounds are small compared to the $q\bar{q}$ continuum events and are studied using MC simulations. We find that no $b \to c$ events pass our selection criteria. The charmless rare background, however, shows peaking structure in the $M_{\rm bc}$ distribution, most of which arises from $B^+ \to \eta\rho^+$ decays.

Correlations among the fit variables are found to be small, and thus we factorize the PDFs as

$$\mathcal{P}_j(M_{\rm bc}, \Delta E, C'_{NB}) = \mathcal{P}_j(M_{\rm bc}) \cdot \mathcal{P}_j(\Delta E) \cdot \mathcal{P}_j(C'_{NB}). \tag{3}$$

All PDFs for C'_{NB} are modeled with the sum of two Gaussian functions. The $M_{\rm bc}$ and ΔE PDFs for signal events are modeled with "crystal ball" (CB) functions [25]. The peak positions and resolutions in the signal $M_{\rm bc}$, ΔE, and C'_{NB} are adjusted according to data-MC differences observed in a high statistics control sample of $B^0 \to \overline{D}^0(\to K^+\pi^-\pi^0)\pi^0$ decays. This decay has four photons, as do signal decays, and its topology is identical to that of $B^0 \to \eta_{3\pi}\pi^0$. The C'_{NB} PDF of the continuum background is also adjusted by comparing data and continuum MC samples in the $M_{\rm bc}$ sideband (5.200-5.265 GeV/c^2). The ΔE PDF for continuum background is modeled with a second-order polynomial, while the $M_{\rm bc}$ PDF is modeled with an ARGUS function [9]. The $M_{\rm bc}$ and ΔE PDFs for charmless rare background are modeled with one-dimensional nonparametric PDFs based on kernel estimation [26]. In addition to the fitted yields Y_j, the $M_{\rm bc}$ and ΔE PDF parameters for continuum background are also floated, except for the end point of the ARGUS function. All other parameters are fixed to the corresponding MC values. To test the stability of the fitting procedure, numerous fits are performed to large ensembles of MC events.

The signal yields obtained from the fits are listed in Table I. The resulting branching fractions are calculated as

$$\mathcal{B}(B^0 \to \eta\pi^0) = \frac{Y_{\rm sig}}{N_{B\bar{B}} \times \epsilon \times \mathcal{B}_\eta}, \tag{4}$$

where $Y_{\rm sig}$ is the fitted signal yield, $N_{B\bar{B}} = (753 \pm 10) \times 10^6$ is the number of $B\overline{B}$ events, ϵ is the signal efficiency as obtained from MC simulations, and $\mathcal{B}_\eta$ is the branching fraction for $\eta \to \gamma\gamma$ or $\eta \to \pi^+\pi^-\pi^0$ [17]. For the latter mode, ϵ is corrected by a factor $\epsilon_{\rm PID} = 0.955 \pm 0.015$ to account for a small difference in particle identification (PID) efficiencies between data and simulations. This correction is estimated from a sample of $D^{*+} \to D^0(\to K^-\pi^+)\pi^+$ decays.

In Eq. (4), we assume equal production of $B^0\overline{B}^0$ and B^+B^- pairs at the $\Upsilon(4S)$ resonance. The combined branching fraction is determined by simultaneously fitting both $B^0 \to \eta_{\gamma\gamma}\pi^0$ and $B^0 \to \eta_{3\pi}\pi^0$ samples for a common $\mathcal{B}(B^0 \to \eta\pi^0)$. Projections of the simultaneous fit are shown in Fig. 2.

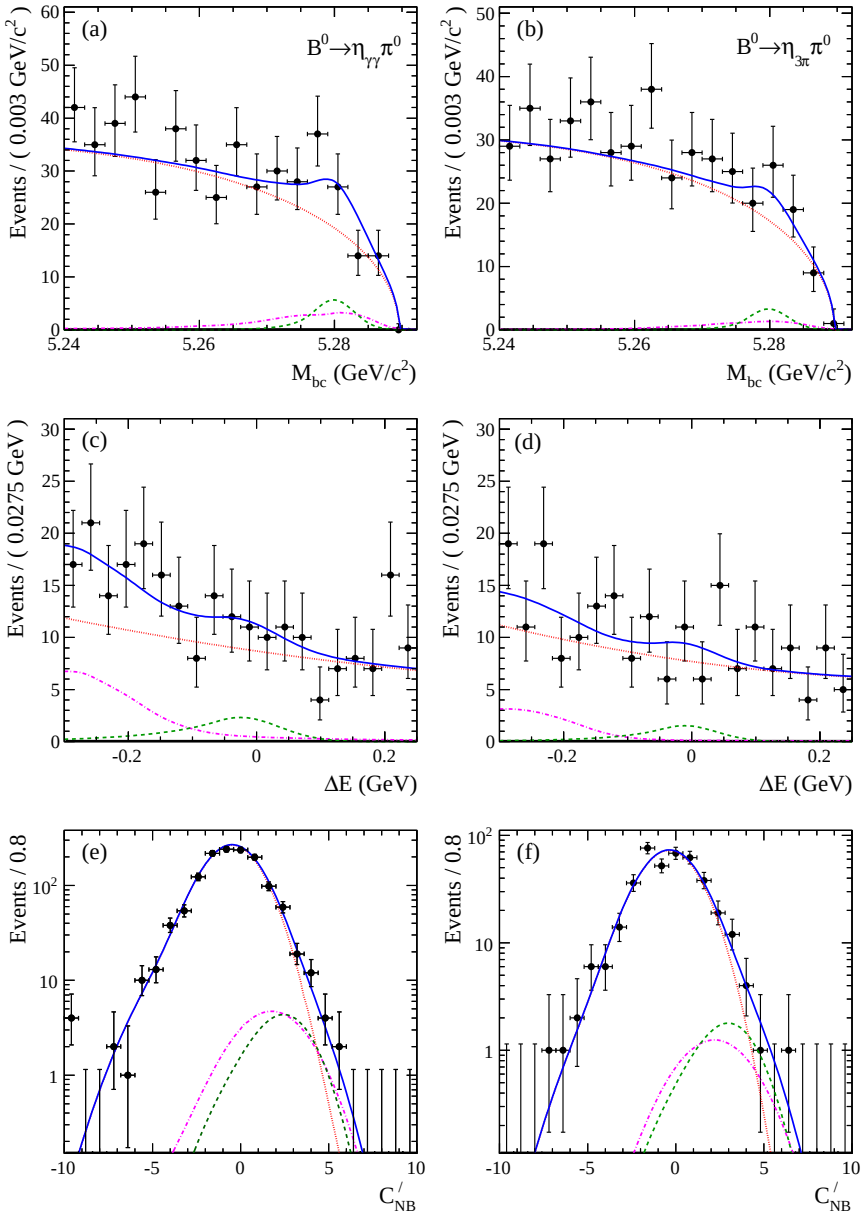

FIG. 2. Projections of the simultaneous fit: (a), (b) $M_{\rm bc}$; (c), (d) ΔE; (e), (f) C'_{NB}. Events plotted in $M_{\rm bc}$ (ΔE) are required to be in the signal region of ΔE ($M_{\rm bc}$), and $C'_{NB} > 1.5$ (0.5) for $\eta_{\gamma\gamma}\pi^0$ ($\eta_{3\pi}\pi^0$) decays. C'_{NB} is plotted in the signal region of $M_{\rm bc}$ and ΔE. The left (right) column corresponds to $\eta \to \gamma\gamma$ ($\eta \to \pi^+\pi^-\pi^0$) decays. Points with error bars are data; the (green) dashed, (red) dotted and (magenta) dot-dashed curves represent the signal, continuum and charmless rare backgrounds, respectively, and the (blue) solid curves represent the total PDF.

The signal significance is calculated as $\sqrt{-2\ln(\mathcal{L}_0/\mathcal{L}_{\rm max})}$, where $\mathcal{L}_0$ is the likelihood value

TABLE I. Fitted signal yield $Y_{\rm sig}$, reconstruction efficiency ϵ, η decay branching fraction $\mathcal{B}_\eta$, signal significance, and B^0 branching fraction $\mathcal{B}$. The errors listed are statistical only. The significance includes both statistical and systematic uncertainties (see text).

Mode	$Y_{\rm sig}$	$\epsilon(\%)$	$\mathcal{B}_\eta(\%)$	Significance	$\mathcal{B}(10^{-7})$
$B^0 \to \eta_{\gamma\gamma}\pi^0$	$30.6^{+12.2}_{-10.8}$	18.4	39.41	3.1	$5.6^{+2.2}_{-2.0}$
$B^0 \to \eta_{3\pi}\pi^0$	$0.5^{+6.6}_{-5.4}$	14.2	22.92	0.1	$0.2^{+2.8}_{-2.3}$
Combined				3.0	$4.1^{+1.7}_{-1.5}$

when the signal yield is fixed to zero, and $\mathcal{L}_{\rm max}$ is the likelihood value of the nominal fit. To include systematic uncertainties in the significance, we convolve the likelihood distribution with a Gaussian function whose width is set to the total systematic uncertainty that affects the signal yield. The resulting significance is 3.0 standard deviations; thus, our measurement constitutes the first evidence for this decay mode. A Bayesian upper limit on the branching fraction is obtained by integrating the likelihood function from zero to infinity; the value that corresponds to 90% of this total area is taken as the 90% C.L. upper limit. The result is $\mathcal{B}(B^0 \to \eta\pi^0) < 6.5 \times 10^{-7}$.

The systematic uncertainty on the branching fraction has several contributions, as listed in Table II. The systematic uncertainty due to the fixed parameters in the PDF is estimated by varying them individually according to their statistical uncertainties. The resulting changes in the branching fraction are added in quadrature and the result is taken as the systematic uncertainty. We evaluate in a similar manner the uncertainty due to errors in the calibration factors. The sum in quadrature of these two contributions constitutes the uncertainty due to PDF parametrization. We perform large ensemble tests in order to verify the stability of our fit model. We find a potential bias of -2.6%, which we attribute to our neglecting small correlations among the fitted observables. We assign a 3% systematic uncertainty for each reconstructed $\eta \to \gamma\gamma$ or $\pi^0 \to \gamma\gamma$ decay [27] . The systematic uncertainty due to the track reconstruction efficiency is 0.35% per track, as determined from a study of partially reconstructed $D^{*+} \to D^0(\to K^0_S\pi^+\pi^-)\pi^+$ decays. A 1.6% uncertainty (0.8% per pion) is assigned due to the PID criteria applied to charged pions in $\eta \to \pi^+\pi^-\pi^0$ decays. We determine the systematic uncertainty due to the C_{NB} selection by applying different C_{NB} criteria and comparing the results with that of the nominal selection. The differences observed are assigned as the systematic uncertainty. The uncertainty due to the number of $B\overline{B}$ pairs is 1.3%, and the uncertainty on ϵ due to MC statistics is 0.4%. The total systematic uncertainty is obtained by summing in quadrature all individual contributions.

In order to check the reliability of the PDFs used for backgrounds, we fit the data in the $M_{\rm bc}$ sideband 5.24-5.26 GeV/c^2, where the end point of the ARGUS function used for the continuum $M_{\rm bc}$ PDF is allowed to float. For all three distributions, $M_{\rm bc}$, ΔE, and C'_{NB}, the MC PDFs give an excellent description of the data. We subsequently fit a sample of MC sideband events constructed with the same admixture of backgrounds as found in the data sideband and obtain signal yields consistent with zero.

To check for potential nonresonant $B^0 \to \gamma\gamma\pi^0$ and $B^0 \to \pi^+\pi^-\pi^0\pi^0$ decays, we relax the η mass requirement and plot the $\gamma\gamma$ and $\pi^+\pi^-\pi^0$ invariant mass distributions (Fig. 3) for events in the $M_{\rm bc}$–ΔE signal region. Significant peaks are observed for $M_{\gamma\gamma} \approx M_\eta$ and

TABLE II. Systematic uncertainties on $\mathcal{B}(B^0 \to \eta\pi^0)$. Those listed in the upper section are associated with fitting for the signal yields and are included in the signal significance and upper limit calculation.

Source	Uncertainty (%)
PDF parametrization	$^{+10.2}_{-\ 9.2}$
Fit bias	$^{+0.0}_{-2.6}$
$\pi^0/\eta \to \gamma\gamma$ reconstruction	6.0
Tracking efficiency	0.3
PID efficiency	0.6
C_{NB} selection efficiency	$^{+2.1}_{-2.2}$
MC statistics	0.4
Nonresonant contributions	$^{+\ 0.0}_{-10.8}$
$\mathcal{B}(\eta \to \gamma\gamma)$	0.5
$\mathcal{B}(\eta \to \pi^+\pi^-\pi^0)$	1.2
Number of $B\overline{B}$ pairs	1.3
Total	$^{+12.2}_{-15.9}$

$M_{\pi^+\pi^-\pi^0} \approx M_\eta$, as expected. The small sidebands indicate no significant contributions from nonresonant decays. We check this quantitatively by requiring that $M_{\gamma\gamma}$ ($M_{\pi^+\pi^-\pi^0}$) be in the sideband 0.45-0.50 GeV/c^2 (0.56-0.58 GeV/c^2) and repeat the fitting procedure. We find $2.2^{+4.8}_{-3.3}$ ($-2.2^{+3.4}_{-2.5}$) signal decays, consistent with zero. To be conservative, we assign a systematic uncertainty due to $B^0 \to \gamma\gamma\pi^0$ nonresonant decays by appropriately scaling this fit result.

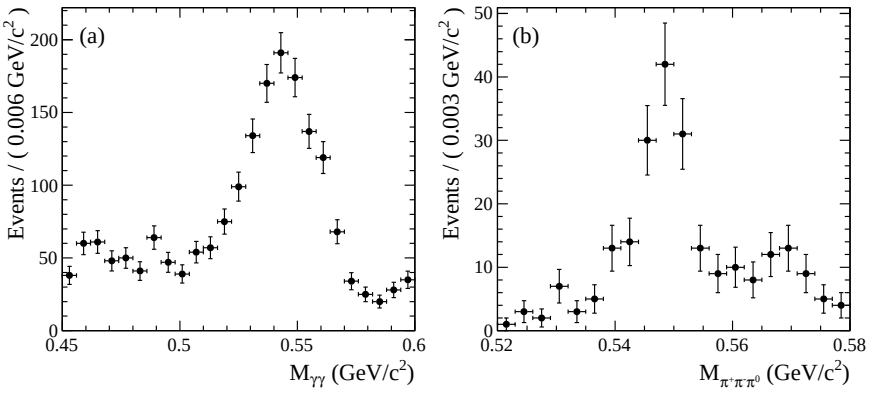

FIG. 3. Distributions of (a) $M_{\gamma\gamma}$ and (b) $M_{\pi^+\pi^-\pi^0}$ invariant masses for events passing all selection requirements, except those for $M_{\gamma\gamma}$ or $M_{\pi^+\pi^-\pi^0}$.

In summary, we report a measurement of the branching fraction for $B^0 \to \eta\pi^0$ decays. We obtain

$$\mathcal{B}(B^0 \to \eta\pi^0) \ = \ \left(4.1^{+1.7+0.5}_{-1.5-0.7}\right) \times 10^{-7},$$

where the first uncertainty is statistical and the second is systematic. This corresponds to a 90% C.L. upper limit of $\mathcal{B}(B^0 \to \eta\pi^0) < 6.5 \times 10^{-7}$. The significance of this result is 3.0 standard deviations, and thus this measurement constitutes the first evidence for this decay. The measured branching fraction is in good agreement with theoretical expectations [6–8]. Inserting our measured value into Eq. (19) of Ref. [3] gives the result that the isospin-breaking correction to the weak phase ϕ_2 measured in $B \to \pi\pi$ decays due to π^0–η–η' mixing is less than 0.97° at 90% C.L.

ACKNOWLEDGMENTS

We thank the KEKB group for the excellent operation of the accelerator; the KEK cryogenics group for the efficient operation of the solenoid; and the KEK computer group, the National Institute of Informatics, and the PNNL/EMSL computing group for valuable computing and SINET4 network support. We acknowledge support from the Ministry of Education, Culture, Sports, Science, and Technology (MEXT) of Japan, the Japan Society for the Promotion of Science (JSPS), and the Tau-Lepton Physics Research Center of Nagoya University; the Australian Research Council and the Australian Department of Industry, Innovation, Science and Research; Austrian Science Fund under Grants No. P 22742-N16 and No. P 26794-N20; the National Natural Science Foundation of China under Contracts No. 10575109, No. 10775142, No. 10875115, No. 11175187, and No. 11475187; the Ministry of Education, Youth and Sports of the Czech Republic under Contract No. LG14034; the Carl Zeiss Foundation, the Deutsche Forschungsgemeinschaft and the VolkswagenStiftung; the Department of Science and Technology of India; the Istituto Nazionale di Fisica Nucleare of Italy; National Research Foundation (NRF) of Korea Grants No. 2011-0029457, No. 2012-0008143, No. 2012R1A1A2008330, No. 2013R1A1A3007772, No. 2014R1A2A2A01005286, No. 2014R1A2A2A01002734, and No. 2014R1A1A2006456; the Basic Research Lab program under NRF Grants No. KRF-2011-0020333 and No. KRF-2011-0021196, Center for Korean J-PARC Users, Grant No. NRF-2013K1A3A7A06056592; the Brain Korea 21-Plus program and the Global Science Experimental Data Hub Center of the Korea Institute of Science and Technology Information; the Polish Ministry of Science and Higher Education and the National Science Center; the Ministry of Education and Science of the Russian Federation and the Russian Foundation for Basic Research; the Slovenian Research Agency; the Basque Foundation for Science (IKERBASQUE) and the Euskal Herriko Unibertsitatea (UPV/EHU) under program UFI 11/55 (Spain); the Swiss National Science Foundation; the National Science Council and the Ministry of Education of Taiwan; and the U.S. Department of Energy and the National Science Foundation. This work is supported by a Grant-in-Aid from MEXT for Science Research in a Priority Area ("New Development of Flavor Physics") and from JSPS for Creative Scientific Research ("Evolution of Tau-lepton Physics").

[1] M. Artuso *et al.*, Eur. Phys. J. C **57**, 309 (2008); M. Antonelli *et al.*, Phys. Rep. **494**, 197 (2010).

[2] Charge conjugate modes are implicitly included unless stated otherwise.

[3] M. Gronau and J. Zupan, Phys. Rev. D **71**, 074017 (2005).

[4] S. Gardner, Phys. Rev. D **72**, 034015 (2005).

[5] M. Gronau, J. L. Rosner and J. Zupan, Phys. Lett. B **596**, 107 (2004); Phys. Rev. D **74**, 093003 (2006).

[6] M. Z. Yang and Y. D. Yang, Nucl. Phys. **B609**, 469 (2001); M. Beneke and M. Neubert, Nucl. Phys. **B675**, 333 (2003); J. f. Sun, G. h. Zhu and D. s. Du, Phys. Rev. D **68**, 054003 (2003); Z. j. Xiao and W. j. Zou, Phys. Rev. D **70**, 094008 (2004); H. s. Wang, X. Liu, Z. j. Xiao, L. b. Guo and C. D. Lu, Nucl. Phys. **B738**, 243 (2006); H. Y. Cheng and C. K. Chua, Phys. Rev. D **80**, 114008 (2009); H. Y. Cheng and J. G. Smith, Annu. Rev. Nucl. Part. Sci. **59**, 215 (2009).
[7] A. R. Williamson and J. Zupan, Phys. Rev. D **74**, 014003 (2006); Phys. Rev. D **74**, 039901 (2006).
[8] C. W. Chiang, M. Gronau and J. L. Rosner, Phys. Rev. D **68**, 074012 (2003); H. K. Fu, X. G. He and Y. K. Hsiao, Phys. Rev. D **69**, 074002 (2004); C. W. Chiang, M. Gronau, J. L. Rosner and D. A. Suprun, Phys. Rev. D **70**, 034020 (2004); C. W. Chiang and Y. F. Zhou, J. High Energy Phys. 12 (2006) 027; H. Y. Cheng, C. W. Chiang and A. L. Kuo, Phys. Rev. D **91**, 014011 (2015).
[9] H. Albrecht *et al.* (ARGUS Collaboration), Phys. Lett. B **241**, 278 (1990).
[10] M. Acciarri *et al.* (L3 Collaboration), Phys. Lett. B **363**, 127 (1995).
[11] S. J. Richichi *et al.* (CLEO Collaboration), Phys. Rev. Lett. **85**, 520 (2000).
[12] P. Chang *et al.* (Belle Collaboration), Phys. Rev. D **71**, 091106 (2005).
[13] B. Aubert *et al.* (BaBar Collaboration), Phys. Rev. D **78**, 011107 (2008).
[14] S. Kurokawa and E. Kikutani, Nucl. Instrum. Methods Phys. Res., Sect. A **499**, 1 (2003), and other papers included in this volume; T. Abe *et al.*, Prog. Theor. Exp. Phys. **2013**, 03A001 (2013) and references therein.
[15] A. Abashian *et al.* (Belle Collaboration), Nucl. Instrum. Methods Phys. Res., Sect. A **479**, 117 (2002); also see the detector section in J.Brodzicka *et al.*, Prog. Theor. Exp. Phys. **2012**, 04D001 (2012).
[16] Z.Natkaniec *et al.* (Belle SVD2 Group), Nucl. Instrum. Methods Phys. Res., Sect. A **560**, 1(2006).
[17] K. A. Olive *et al.* (Particle Data Group), Chin. Phys. C **38**, 090001 (2014).
[18] M. Feindt and U. Kerzel, Nucl. Instrum. Methods Phys. Res., Sect. A **559**, 190 (2006).
[19] H. Kakuno *et al.*, Nucl. Instrum. Methods Phys. Res., Sect. A **533**, 516 (2004).
[20] The Fox-Wolfram moments were introduced in G. C. Fox and S. Wolfram, Phys. Rev. Lett. **41**, 1581 (1978). The Fisher discriminant used by Belle, based on modified Fox-Wolfram moments, is described in K. Abe *et al.* (Belle Collaboration), Phys. Rev. Lett. **87**, 101801 (2001) and K. Abe *et al.* (Belle Collaboration), Phys. Lett. B **511**, 151 (2001).
[21] S. Brandt, C. Peyrou, R. Sosnowski and A. Wroblewski, Phys. Lett. **12**, 57 (1964).
[22] D. J. Lange, Nucl. Instrum. Methods Phys. Res., Sect. A **462**, 152 (2001).
[23] R. Brun *et al.*, GEANT 3.21, CERN Report DD/EE/84-1, 1984.
[24] P. Golonka and Z. Wąs, Eur. Phys. J. C **45**, 97 (2006).
[25] T. Skwarnicki, Ph.D. thesis, Institute of Nuclear Physics, Krakow, 1986, DESY-F31-86-02.
[26] K. S. Cranmer, Comput. Phys. Commun. **136**, 198 (2001).
[27] M. C. Chang *et al.* (Belle Collaboration), Phys. Rev. D **85**, 091102(R) (2012).